2009 American Control Conference
Hyatt Regency Riverfront, St. Louis, MO, USA
June 10-12, 2009

Laser Beam Pointing and Stabilization by Intensity Feedback Control

Néstor O. Pérez-Arancibia, James S. Gibson and Tsu-Chin Tsao

Abstract— **This paper presents an investigation of the control problem of aiming a laser beam under dynamic disturbances, using light intensity for feedback. The beam is steered with a bi-axial MEMS mirror, which is driven by a control signal generated by processing the beam intensity sensed by a single photodiode. Since the pointing location of the beam is assumed to be not available for real-time control, a static nonlinear mapping from the two-dimensional beam location to the sensor measurement is estimated with the use of the least-squares algorithm, using data from an *optical position sensor* (OPS). The previous formulation results in a state-space system model with a nonlinear output function. The controller design problem is addressed with the integration of an *extended Kalman filter* (EKF) and a pair of *linear time-invariant* (LTI) *single-input/single-output* (SISO) controllers into one system. In order to demonstrate the effectiveness of the proposed approach, experimental results of a case relevant to free-space optics for communications and directed energy applications is presented here.**

I. Introduction

Laser beams are used to transmit information or energy in a wide range of applications, from laser cutting to metrology, from laser surgery to communications. Applications typically require the beam to aim at a target with a maximum possible light intensity level, or above a specified threshold value, traveling through free space, the atmosphere or other transmissible media, while subjected to disturbances from multiple sources. In most beam control systems, bi-axial sensors, such as, OPSs, *charge-coupled devices* (CCDs) or quad-photo detectors, are used to determine the coordinated location of the beam projection on a plane, which is fedback into a two-input/two-output controller (e.g., see [1], [2], [3] and references therein).

In many applications, single photodiode sensors are currently being used for purposes other than feedback control in where tracking is not attempted because the use of coordinate sensors is not convenient due to cost, space or other technical reasons. Thus, the possibility of using single photodiode sensors for feedback control is of great interest, since this might significantly increase the overall performance and reliability of some important optical systems. A possible application of feedback control based on single photodiode sensors arises in the area of free-space laser communications. There, laser beams are modulated at frequencies significantly higher than the frequencies of the surrounding disturbances, in order to encode and transmit data. In those systems, there are optical links that require that a sufficient amount of laser power reaches the receiver end, so that, data loss is minimized during the decoding process.

A method to approach the problem, based on the notion of nutation, is presented in [4]. There, a small high-frequency nutation signal is inputed to the system, inducing a known, or estimable, additional tracking error, used for determining the spatial position of the laser beam center. If implemented in discrete-time, this method requires extremely high sampling rates. Another approach, and a matter of further research, is the implementation of some kind of real-time optimization algorithm, based on methods such as artificial neural networks [5] or extremum seeking control [6].

A third approach, the one considered here, is the implementation of an observer-based controller. In this case, we employ an EKF [7], [8] to estimate the bi-dimensional position of the laser beam center on an imaginary plane, using the intensity measurement obtained from a single photodiode sensor. Then, the estimated coordinates are used to generate a control signal by means of a pair of SISO LTI controllers. This is reasonable, because the original control objective is to maximize the light intensity detected by the photodiode sensor, and this objective is equivalent to position the laser beam center at a specific position over an imaginary coordinated plane where the light intensity is maximized. It is known that the relationship between position coordinates and intensity can be approximated by a quadratic static function [4].

Here, a static mapping is estimated using the least-squares algorithm from $450,000$ data samples obtained using a bi-axial OPS and the photodiode sensor employed for control. The EKF is a heuristic solution, and therefore, there is no guarantee of optimality, or even, functionality. The experimental results presented here suggest that it is not possible to steer the system to the desired optimal operation point. However, we show empirically that the laser beam can be steered to suboptimal operation points, improving the overall performance of the optical system significantly, because a noticeable amount of disturbance can be rejected. This could be of great utility in many applications. For example, in laser communications, the power at the receiving end of an optical link is required to be above a specified threshold value in order to maintain the communication link. Therefore, it is more desirable that the sensor receives an amount of light above a specified value at each time instant than it is that the sensor receives a large amount of light at sporadic time instants.

The paper is organized as follows. Section II describes the experiment. Section III reviews some fundamental aspects

This work was supported by the Office of Naval Research under Grant N00014-07-1-1063.

The authors are with the Mechanical and Aerospace Engineering Department, University of California, Los Angeles, CA, 90095–1597, USA. nestor@seas.ucla.edu, gibson@ucla.edu, ttsao@seas.ucla.edu.

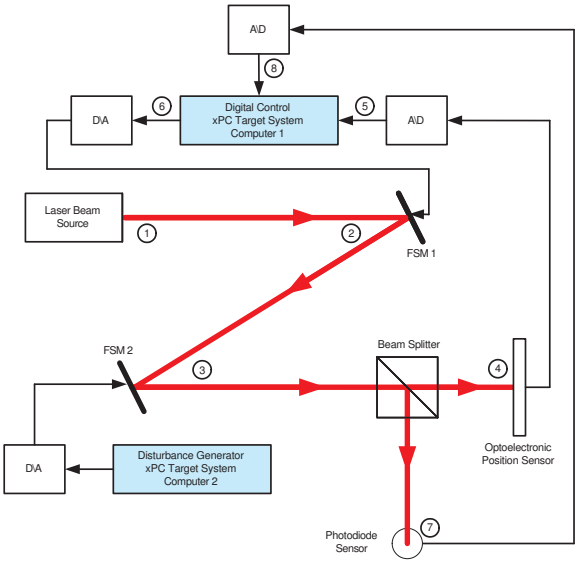

Fig. 1. Diagram of the experiment.

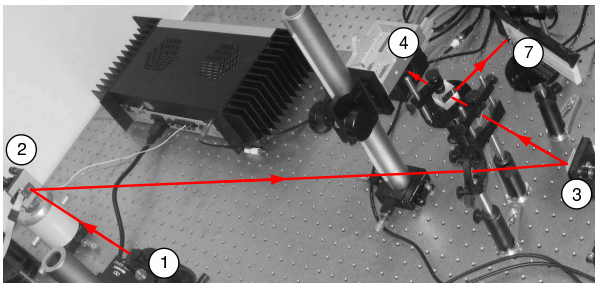

Fig. 2. Optical bench with optical path.

of the EKF. Section IV describes the proposed method for designing observer-based controllers and discusses the implementation of light intensity feedback control schemes for laser beam tracking. Section V presents experimental results, and finally, Section VI draws some conclusions.

II. Description of the Experiment

The experiment considered in this paper is shown in the block diagram in Fig. 1 and in the photograph in Fig. 2. There, a laser beam is generated with a laser source at position ①. Immediately after, the laser beam reflects off the bi-axial fast steering mirror FSM 1 at position ②, then it reflects off the bi-axial fast steering mirror FSM 2 at position ③ and before reaching positions ④ and ⑦ it is split using a non-polarizing beamsplitter cube. At positions ④ and ⑦, a two-dimensional OPS and a single photodiode sensor are located, respectively. FSM 1 and FSM 2 are identical *Texas Instruments* (TI) MEMS mirrors used in laser communications for commercial and defense applications, and the OPS is an On-Track sensing device. FSM 1 is used for control actuation and FSM 2 is used for generating jitter, which disturbs the laser beam horizontally and vertically. A second source of jitter is a shaker with vertical motion on which the control actuator FSM 1 is mounted. The shaker is used for introducing disturbances with narrow frequency bands, recreating the effects of vibrating platforms over which real-life optical systems are mounted.

The OPS determines the coordinates of the laser beam spot center on the sensor, and then, these measurements, in the form of voltages, go to Computer 1. As described in [2] and papers therein, high performance position feedback controllers, based on LTI, adaptive or other methods, can be designed and implemented using the almost-perfect coordinate location information provided by optical position sensors. In this work, OPS measurements are used for monitoring and identification purposes, but not for control. Feedback control is performed using only the light intensity measurement generated by the single photodiode sensor at position ⑦. Computer 1 runs the feedback controller that generates and sends actuator commands to FSM 1. Computer 2 sends disturbance commands to FSM 2 and to the shaker. The sampling and computing rate, to which the digital controller and the disturbance generator are run, is 5 KHz.

In the rest of the paper, P is the open-loop LTI transfer function that maps the two-channel digital control command, marked by ⑥ in Fig. 1, to the sampled two-channel position sensor output, marked by ⑤ in Fig. 1. Thus, P is the two-input/two-output digital transfer function for FSM 1 with a gain determined by the OPS and the laser path length. Output channels 1 and 2 represent horizontal and vertical displacements, respectively, of the beam. Input channels 1 and 2 represent commands that drive FSM 1 about its vertical and horizontal axes, respectively. Input-output data from open-loop experiments showed negligible coupling between the two channels of P, so henceforth, all discussion assumes that P has two uncoupled channels, labeled as P_1 and P_2, respectively. An estimate $\hat{P}$ of P was identified as in [3]. The corresponding Bode plot is shown in Fig. 3.

For purposes of analysis, a classical LTI two-input/two-output controller K, to be connected to P according to Fig. 4, is designed as in [3]. The output disturbance n represents the combined effects of all disturbances acting on the system. The two-channel sensitivity function, mapping n to z, for the closed-loop LTI system is

$$S = (I + PK)^{-1}, \tag{1}$$

$$P = \begin{bmatrix} P_1 & 0 \\ 0 & P_2 \end{bmatrix}, \quad K = \begin{bmatrix} K_1 & 0 \\ 0 & K_2 \end{bmatrix}. \tag{2}$$

An estimate of S, $\hat{S} = \left(I + \hat{P}K\right)^{-1}$, is shown in Fig. 3.

The controller K, directly connected to P as in Fig. 4, is not used in the experiment presented here. However, both systems $\hat{P}$ and K are used in the design of the observer-based controller, which uses only light intensity for feedback. The mapping from the two-channel digital control command, marked by ⑥ in Fig. 1, to the sampled single photodiode sensor output, marked by ⑧ in Fig. 1, is a two-input/one-output nonlinear dynamical system. This nonlinear system can be thought of as the LTI plant P connected in series to

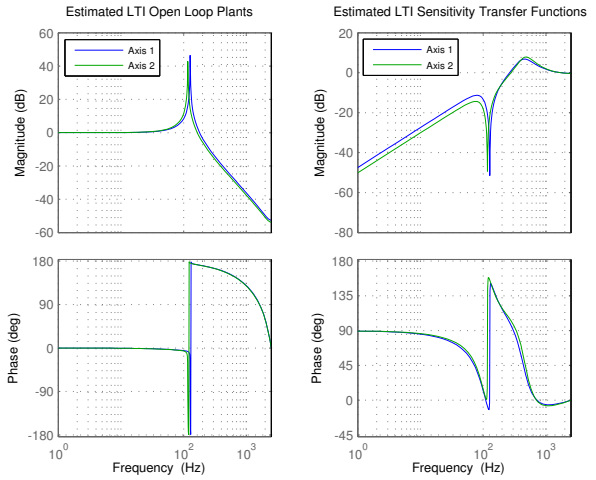

Fig. 3. *Left Plot:* Bode plots of estimated LTI open-loop plants $\hat{P}_1$ and $\hat{P}_2$. *Right Plot:* Bode plots of estimated LTI output sensitivity functions $\hat{S}_1 = (1+\hat{P}_1 K_1)^{-1}$ and $\hat{S}_2 = (1+\hat{P}_2 K_2)^{-1}$, where $\hat{S} = \left[\hat{S}_1\ 0;\ 0\ \hat{S}_2\right]$.

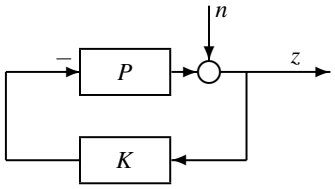

Fig. 4. Configuration used in the design of the two-input/two-output LTI controller K. P: LTI two-input/two-output open-loop plant; n: output disturbance; z: two-dimensional laser beam spot position on the OPS.

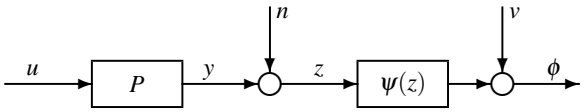

Fig. 5. Idealization of the two-input/one-output open-loop nonlinear system mapping the FSM 1 input commands to the photodiode sensor output. P: LTI open-loop plant; $\psi(z)$: static map; u: input command to FSM 1; y: output from LTI open-loop plant P; n: output disturbance; z: two-dimensional laser beam spot position on the OPS; v: sensor noise; ϕ: photodiode sensor output.

a static mapping that maps the coordinates measured using the OPS to the output from the single photodiode sensor in Fig. 5. Photodiodes are solid-state devices that convert light into voltage. Thus, the output from the photodiode sensor at position ⑦ is measured in volts and is linearly related to light intensity units. Since this relation is linear, in this work we ignore the unit transformation, and therefore, the control implementation and the data analysis are conducted using units of voltage.

III. Review of the Extended Kalman Filter

Since the replacement of the OPS by a photodiode transforms the measurement process from linear to nonlinear, the problem described in Section II leads to a nonlinear filtering problem. In general, a nonlinear dynamic system can be written as

$$x(t+1) = f(x(t), w(t)), \tag{3}$$
$$\phi(t) = g(x(t), v(t)), \tag{4}$$

where f and g are possibly nonlinear functions, and w and v are stationary zero-mean white random processes with

$$E\begin{bmatrix} w(t) \\ v(t) \\ x(0)-\bar{x}_0 \end{bmatrix}\begin{bmatrix} w(t) \\ v(t) \\ x(0)-\bar{x}_0 \end{bmatrix}^T = \begin{bmatrix} \Sigma_w & 0 & \\ 0 & \Sigma_v & 0 \\ 0 & 0 & \Sigma_0 \end{bmatrix}, \tag{5}$$

where $\bar{x}_0 = E[x(0)]$.

Regardless of the model, the least-mean-squares predictor of the state vector $x(t)$, based on the past observed outputs, and the least-mean-squares estimator of the state vector $x(t)$, based on the current and past observed outputs, at any particular time instant t, are given by the conditional means [8], [7], i.e.,

$$\hat{x}(t|t-1) = E[x(t)|\Phi(t-1)], \tag{6}$$
$$\hat{x}(t|t) = E[x(t)|\Phi(t)], \tag{7}$$

where $\Phi(t-1) = \{\phi(\sigma),\ 0<\sigma<t-1\}$ and $\Phi(t) = \{\phi(\sigma),\ 0<\sigma<t\}$.

Finding explicit formulas for (6) and (7) is almost always very difficult. A heuristic approach to this problem is the EKF [8], [7], which is based on linearizing the dynamics and output functions at current estimate, and on propagating an approximation of the conditional expectation and covariance. The resulting algorithm as presented in [7] is as follows.

Algorithm 1 (EKF). Consider the model (3)–(4) with conditions (5). An approximate estimator for the state $x(t)$ can be recursively computed as follows.

- initialization: $\hat{x}(0|-1) = \bar{x}_0$, $\Sigma_{0|-1} = \Sigma_0$.
- linearize output function at $x = \hat{x}(t|t-1)$:

$$\zeta = \frac{\partial g}{\partial x}(\hat{x}(t|t-1), 0), \tag{8}$$
$$V = \frac{\partial g}{\partial v}(\hat{x}(t|t-1), 0)\,\Sigma_v \left[\frac{\partial g}{\partial v}(\hat{x}(t|t-1), 0)\right]^T. \tag{9}$$

- measurement update based on linearization:

$$\hat{x}(t|t) = \hat{x}(t|t-1) + \kappa_t\left(\phi(t) - g(\hat{x}(t|t-1), 0)\right), \tag{10}$$
$$\Sigma_{t|t} = \Sigma_{t|t-1} - \kappa_t \zeta \Sigma_{t|t-1}, \tag{11}$$

with

$$\kappa_t = \Sigma_{t|t-1}\zeta^T\left(\zeta\Sigma_{t|t-1}\zeta^T + V\right)^{-1}. \tag{12}$$

- linearize dynamics function at $x = \hat{x}(t|t)$:

$$A = \frac{\partial f}{\partial x}(\hat{x}(t|t), 0), \tag{13}$$
$$W = \frac{\partial f}{\partial w}(\hat{x}(t|t), 0)\,\Sigma_w \left[\frac{\partial f}{\partial w}(\hat{x}(t|t), 0)\right]^T. \tag{14}$$

- time update based on linearization:

$$\hat{x}(t+1|t) = f(\hat{x}(t|t), 0), \tag{15}$$
$$\Sigma_{t+1|t} = A\Sigma_{t|t}A^T + W. \tag{16}$$

□

IV. Observer-based Controller Design

In order to design an appropriate observer, we consider the idealized block diagram in Fig. 6, which shows the interaction between all the subsystems involved. There, P_1 and P_2 represent the discrete-time open-loop LTI systems corresponding to the Axis 1 and Axis 2 of the actuator MEMS mirror, respectively. The systems K_1 and K_2 are LTI controllers designed under the assumption that $\hat{z}_1 = z_1$ and $\hat{z}_2 = z_2$. The function ψ is the mapping from the two-dimensional position of the laser beam spot on the OPS to the noise-free light intensity measurement from the photodiode. The inputs to the observer are the inputs to P_1 and P_2 and the noisy light intensity measurement ϕ. The outputs from the observer are estimates for the position signals z_1 and z_2. The output disturbances n_1 and n_2 represent the aggregated effects of all the disturbances injected to the optical system by FSM 2 and by the shaker. Similarly, the signal v represents the aggregated effects of physical sensor noise in the photodiode and mismatch between the true and idealized mappings ψ. Finally, r_1 and r_2 are position references generated inside the digital signal processor.

The observer design assumes the LTI disturbance models

$$n_1 = N_1 w_{N_1}, \quad n_2 = N_2 w_{N_2}, \tag{17}$$

where w_{N_1} and w_{N_2} are stationary zero-mean white random processes. Notice that the parameters defining the filters N_1 and N_2 will become design parameters of the observer, and therefore, an a priori exact knowledge of N_1 and N_2 will not be needed in practice. Also for purposes of design, v is assumed to be stationary, zero-mean and white, and the mapping ψ is considered to quadratic, i.e.,

$$\psi(z_1, z_2) = a_1 z_1^2 + a_2 z_2^2 + a_{12} z_1 z_2 + b_1 z_1 + b_2 z_2 + c. \tag{18}$$

Thus, considering Fig. 6, (17) and (18) the open-loop nonlinear model to be employed in the design of the observer is given by

$$x(t+1) = A_\phi x(t) + B_w w(t) + B_u u(t), \tag{19}$$

$$z(t) = \begin{bmatrix} z_1(t) \\ z_2(t) \end{bmatrix} = C_\phi x(t), \tag{20}$$

$$\phi(t) = \psi(z_1(t), z_2(t)) + v(t), \tag{21}$$

where

$$A_\phi = \begin{bmatrix} A_{P_1} & 0 & 0 & 0 \\ 0 & A_{N_1} & 0 & 0 \\ 0 & 0 & A_{P_2} & 0 \\ 0 & 0 & 0 & A_{N_2} \end{bmatrix}, \tag{22}$$

$$B_w = B_u = \begin{bmatrix} B_{P_1} & 0 & 0 & 0 \\ 0 & B_{N_1} & 0 & 0 \\ 0 & 0 & B_{P_2} & 0 \\ 0 & 0 & 0 & B_{N_2} \end{bmatrix}, \tag{23}$$

$$C_\phi = \begin{bmatrix} C_{P_1} & C_{N_1} & 0 & 0 \\ 0 & 0 & C_{P_2} & C_{N_2} \end{bmatrix}. \tag{24}$$

The sets of matrices $\{A_{P_1}, B_{P_1}, C_{P_1}\}$, $\{A_{P_2}, B_{P_2}, C_{P_2}\}$, $\{A_{N_1}, B_{N_1}, C_{N_1}\}$ and $\{A_{N_2}, B_{N_2}, C_{N_2}\}$ define state-space

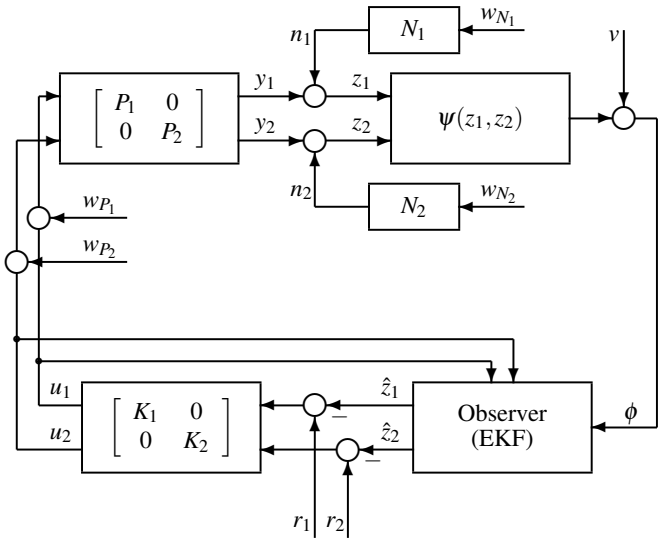

Fig. 6. Signals-and-systems block diagram idealization of the optical system with proposed control scheme.

realizations for the systems P_1, P_2, N_1 and N_2, respectively. The signals $w(t)$ and $u(t)$ are formed as

$$w(t) = \begin{bmatrix} w_{P_1}(t) \\ w_{N_1}(t) \\ w_{P_2}(t) \\ w_{N_2}(t) \end{bmatrix}, \quad u(t) = \begin{bmatrix} u_1(t) \\ 0 \\ u_2(t) \\ 0 \end{bmatrix}, \tag{25}$$

where w_{P_1} and w_{P_2} are stationary zero-mean white random processes, inputs to P_1 and P_2, respectively. Similar to w_{N_1} and w_{N_2}, w_{P_1} and w_{P_2} are assumed for design purposes, but those are not necessarily true signals driving the system. The signals u_1 and u_2 are deterministic known signals generated inside the digital signal processor, using controller K.

Notice that since (19) depends on $u(t)$, the form of (19) is slightly different from the form of (3). However, this will not modify the EKF design algorithm significantly, because $u(t)$ is known by the observer. Thus, the only thing to change is the way in which the system state estimate is time-updated, i.e., (15) is replaced by

$$\hat{x}(t+1|t) = f(\hat{x}(t|t), 0, u(t)) = A_\phi \hat{x}(t|t) + B_u u(t). \tag{26}$$

Now, the only things remaining to be found and incorporated in the design, are relations for ζ, V, A and W according to (8), (9), (13) and (14). To begin with ζ, define matrices C_1 and C_2 as

$$C_1 = \begin{bmatrix} C_{11} & C_{12} & C_{13} & \cdots \end{bmatrix} = \begin{bmatrix} C_{P_1} & C_{N_1} \end{bmatrix}, \tag{27}$$

$$C_2 = \begin{bmatrix} C_{21} & C_{22} & C_{23} & \cdots \end{bmatrix} = \begin{bmatrix} C_{P_2} & C_{N_2} \end{bmatrix}, \tag{28}$$

where C_{1i} is the ith entry of the row vector C_1 and C_{2i} is the ith entry of the row vector C_2. Also, partition the system state vector as

$$x(t) = \begin{bmatrix} x_1(t) \\ x_2(t) \end{bmatrix}, \tag{29}$$

according the dimensions of C_1 and C_2, i.e., $x_1(t)$ has the same number of elements as C_1 and $x_2(t)$ has the same

number of elements as C_2. Then, define

$$\psi_1(x_1(t)) = C_1 x_1(t), \quad \psi_2(x_2(t)) = C_2 x_2(t). \tag{30}$$

It immediately follows that

$$\begin{aligned}\phi(t) = {} & a_1\psi_1^2(x_1(t)) + a_2\psi_2^2(x_2(t)) \\ & + a_{12}\psi_1(x_1(t))\psi_2(x_2(t)) \\ & + b_1\psi_1(x_1(t)) + b_2\psi_2(x_2(t)) + c + v(t),\end{aligned} \tag{31}$$

$$\frac{\partial\phi}{\partial x_{1i}} = 2a_1C_{1i}\psi_1 + b_1C_{1i} + a_{12}C_{1i}\psi_2, \tag{32}$$

$$\frac{\partial\phi}{\partial x_{2i}} = 2a_2C_{2i}\psi_2 + b_2C_{2i} + a_{12}C_{2i}\psi_1, \tag{33}$$

which implies that ζ, according to (8), is given by

$$\zeta = \begin{bmatrix} \zeta_1 & \zeta_2 \end{bmatrix}, \text{ with} \tag{34}$$

$$\zeta_1 = [2a_1\psi_1(\hat{x}_1(t|t-1)) + b_1 + a_{12}\psi_2(\hat{x}_1(t|t-1))]C_1, \tag{35}$$

$$\zeta_2 = [2a_2\psi_2(\hat{x}_2(t|t-1)) + b_2 + a_{12}\psi_1(\hat{x}_2(t|t-1))]C_2. \tag{36}$$

Similarly, we obtain

$$V = \Sigma_v, \quad A = A_\phi, \quad W = B_w\Sigma_w B_w^T, \tag{37}$$

which completes the observer design.

V. Experimental Results

A photodiode is a semiconductor light sensor that generates a current or voltage when its P-N junction is illuminated by light, making possible the detection of intensity of light [9]. In the experiment described here, a HAMAMATSU S6468 photodiode, connected in the basic form, is utilized to generate a voltage related by a linear function with negative slope to intensity of light. Since the slope of the linear relation is negative, when the light intensity increases the photodiode output voltage decreases. Thus, if no light is incidenting the photodiode sensor surface, the voltage output is a positive number greater than zero. Conversely, if the amount of light illuminating the photodiode sensor surface is too great, the sensor saturates and the voltage output is equal to zero. With this in mind, in this work we ignore the unit transformation, and therefore, the control implementation and the data analysis are conducted using units of voltage. Notice that by using the photodiode sensor voltage output for feedback, the mapping ψ becomes a convex function, and therefore, the optimal operation point is the closest point in the surface determined by ψ to the plane $\{z_1 = 0, z_2 = 0\}$. An estimate of the mapping $\psi(z_1, z_2)$ computed using the minimum least-squares method, employing $450,000$ data samples, is shown in Fig. 7.

As explained in the previous sections, the proposed controller consists of two fundamental subsystems: an EKF-based observer as described in Section IV and the LTI controller K described in Section II. Recalling that the LTI rejection bandwidth of K is about 200 Hz, this bandwidth determines the limiting performance of the EKF-based controller as well. Thus, in order to test the proposed controller, the disturbance injected to the optical system has a frequency contend below 200 Hz. The disturbance for channel 1 is generated using FSM 2, resulting in a signal whose spectrum has fundamentally three frequency bands: 0–50 Hz, 112–118 Hz, 122–132 Hz. The disturbance for channel 2 is generated using FSM 2 and the shaker, resulting in a signal whose spectrum has fundamentally three frequency bands: 0–5 Hz, 100–108 Hz, 115–125 Hz and two peaks: 20 Hz, 40 Hz. The selection of these disturbances is arbitrary.

As shown in Fig. 8, the controller is able to reject the disturbance affecting the optical system significantly. There, the top plot shows the photodiode voltage output comparing the cases in which the system is and is not under control. The middle and bottom plots show the monitoring signals z_1 and z_2 obtained by the use of the optical position sensor. It is important to remark that the controller is implemented using the photodiode output ϕ and that z_1 and z_2 are used for analysis only.

A second important thing to notice in Fig. 8 is that the controlled optical system does not operate at the optimal point. The explanation for that is that the EKF observer can only function if the reference signals r_1 and r_2 introduce a bias with respect to the optimal operation point. Heuristically speaking, this is because given that the mapping ψ is quadratic, the observer needs to "know" the average position of the laser spot on the plane. This information is contained in the input signals u_1 and u_2. Notice that the smaller the standard deviation of ϕ, the smaller the bias introduced by r_1 and r_2 can be. As it can be observed in the plots in Fig. 8, the control loop is closed at Time = 10 secs, and then, the reference signals r_1 and r_2 drive the system closer to the optimal operation point. In this case it is clear that the systems operates robustly. However, if signals r_1 and r_2 are moved closer to the optimal operation point, the system would go unstable. Since the solution presented here is heuristic, the election of appropriate reference signals r_1 and r_2 is heuristic as well.

The steady-state performance of the control system, in this particular experiment, is graphically summarized by the plots in Fig. 9. There, the left plot shows the histograms of the photodiode output ϕ comparing the cases in which the system is and is not under control. The plot on the right shows the monitoring signals z_1 and z_2 on the OPS plane. These plots clearly show that the controller is able to concentrate the values of ϕ closer to the optimal point, and consequently, the guaranteed amount of light at each time instant captured by photodiode sensor is significantly increased.

Figure 10 shows the effect of the controller on the spectrum of the monitoring signals z_1 and z_2. Since a bias is injected to the system when the system is under control, the plots show the *power spectral densities* (PSD) of the signals $z_1 - mean(z_1)$ and $z_2 - mean(z_2)$ comparing the cases in which the system is and is not under control. There, it is clear that from an output disturbance viewpoint, the controller is able to reject a significant amount of disturbance power below 200 Hz.

Finally in this section, it is important to remark that the re-

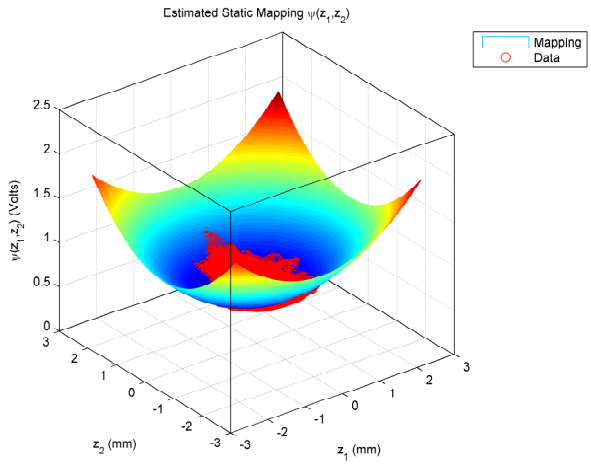

Fig. 7. Estimated static mapping $\psi(z_1, z_2)$, computed using the minimum least-squares algorithm, employing 450,000 data samples. The plot also shows some of the data samples used in the estimation.

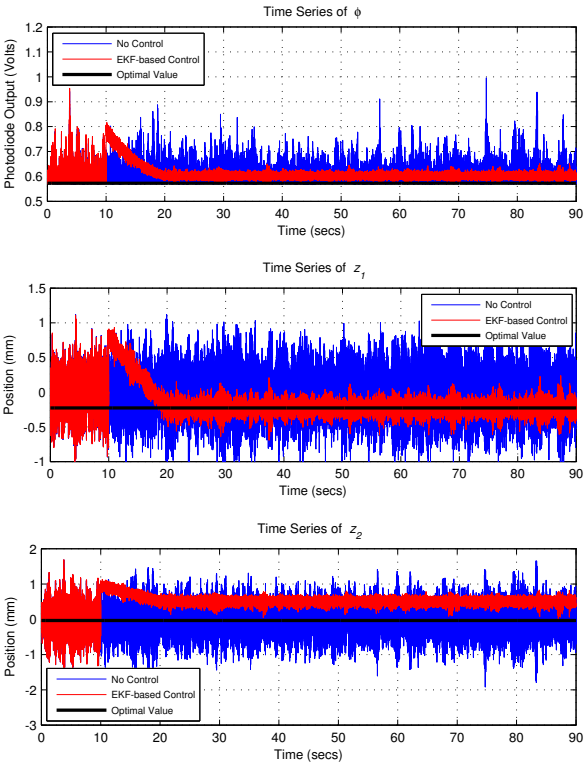

Fig. 8. *Upper Plot:* time series of photodiode output ϕ. *Middle Plot:* time series of position signal z_1. *Bottom Plot:* time series of position signal z_2.

sults presented here depend on the tuning parameters Σ_w, Σ_v, the disturbance models N_1 and N_2 and the initial conditions of the EKF observer. Therefore, designs employing different parameters, disturbance models and initial conditions would produce different experimental results.

VI. Conclusions

This paper presented an investigation of the control problem of aiming a laser beam, using a single photodiode output voltage for feedback. The proposed controller is designed

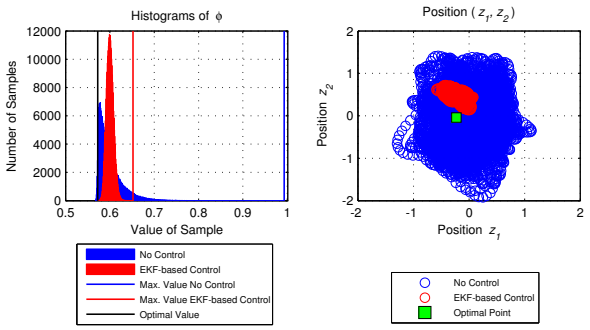

Fig. 9. *Left Plot:* histograms of photodiode output ϕ. *Right Plot:* two-dimensional position of the laser beam spot.

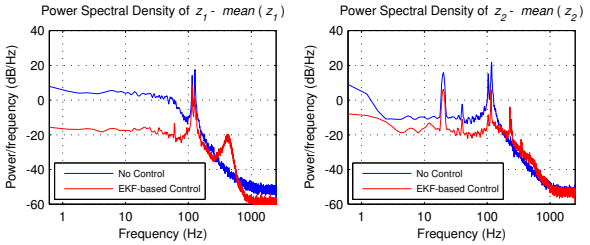

Fig. 10. *Left Plot:* PSD of $z_1 - mean(z_1)$. *Right Plot:* PSD of $z_2 - mean(z_2)$.

with the objective of rejecting disturbances acting on the optical system and ensuring connectivity of the optical path, by guaranteeing a given amount of light on the surface of the photodiode detector. The proposed control scheme consists of two subsystems: a LTI controller designed using classical techniques and an observer designed using the extended Kalman filter method. The main innovation of this work is the augmentation of the state-space of the open-loop system, including LTI models for the output disturbances acting on the system, as a design technique.

References

[1] M. A. McEver, D. G. Cole, and R. L. Clark, "Adaptive feedback control of optical jitter using *Q*–parameterization," *Optical Engineering*, vol. 43, no. 4, pp. 904–910, Apr. 2004.

[2] N. O. Pérez Arancibia, N. Chen, S. Gibson, and T.-C. Tsao, "Variable-order adaptive control of a microelectromechanical steering mirror for suppression of laser beam jitter," *Optical Engineering*, vol. 45, no. 10, pp. 104 206–1–12, Oct. 2006.

[3] N. O. Pérez-Arancibia, J. S. Gibson, and T.-C. Tsao, "Frequency-Weighted Minimum-Variance Adaptive Control of Laser Beam Jitter," *Accepted for publication in IEEE/ASME Transactions on Mechatronics*, available at http://www.seas.ucla.edu/∼nestor/publications.htm.

[4] T. E. Knibbe, *Spatial Tracking using an Electro-Optic Nutator and a Single-Mode Optical Fiber*. Cambridge, MA: M.S. Thesis, Massachusetts Institute of Technology, 1993.

[5] G. L. Plett, "Adaptive Inverse Control of Linear and Nonlinear Systems Using Dynamic Neural Networks," *IEEE Transactions on Neural Networks*, vol. 14, no. 2, pp. 360–376, Mar. 2003.

[6] K. B. Ariyur and M. Krstić, *Real-Time Optimization by Extremum-Seeking Control*. Hoboken, NJ: Wiley, 2003.

[7] S. Boyd, *Lecture Notes EE363 – Linear Dynamical Systems*. Available online at http://www.stanford.edu/class/ee363/.

[8] T. Kailath, A. H. Sayed, and B. Hassibi, *Linear Estimation*. Upper Saddle River, NJ: Prentice Hall, 2000.

[9] Hamamatsu Corporation, *Photodiode Technical Guide*. Available online at http://sales.hamamatsu.com/assets/html/ssd/si-photodiode/index.htm.